Physics of Fluids ARTICLE scitation.org/journal/phf

On the consistent modeling of shear-thickening polymer solutions

Cite as: Phys. Fluids 33, 063107 (2021); doi: 10.1063/5.0053604
Submitted: 9 April 2021 · Accepted: 28 May 2021 ·
Published Online: 24 June 2021

View Online Export Citation CrossMark

Pavlos S. Stephanou[a]

AFFILIATIONS

Department of Chemical Engineering, Cyprus University of Technology, P.O. Box 50329, 3603 Limassol, Cyprus

[a]Author to whom correspondence should be addressed: pavlos.stefanou@cut.ac.cy. Tel.: +357-25-002394. Fax: +357-25-002668

ABSTRACT

During the past few decades, the interest in understanding the peculiar rheological behavior of shear-thickening fluids has increased due to their potential use in various commercial applications. In such an endeavor, the optimal design of these fluids is essential, which necessitates our in-depth understanding of their properties from a modeling perspective. We herein introduce a continuum model to predict the rheological behavior of shear-thickening polymer solutions using non-equilibrium thermodynamics that guarantees, by construction, consistency with the laws of thermodynamics as extended to handle non-equilibrium systems. This is made possible by using a scalar structural variable that characterizes the formation of the shear-induced structure at sufficiently high shear rates, and a conformation tensor that characterizes the deformation of the polymer segments. The model predicts the exhibition of a shear-thickening behavior for all steady shear flow material functions (shear viscosity and normal stress coefficients), which is then followed by a shear-thinning behavior if finite extensibility or anisotropic effects are considered. We further document that these model predictions are in line with available shear viscosity rheological data for shear-thickening polymer solutions.

Published under an exclusive license by AIP Publishing. https://doi.org/10.1063/5.0053604

I. INTRODUCTION

A dilatant or shear-thickening fluid (STF) is a fluid whose viscosity increases with the shear rate.[1] At low shear rates, STF approaches a Newtonian plateau, but its viscosity increases dramatically when the shear rate exceeds a critical value; this behavior is reversible as once the applied flow is removed, the fluid relaxes and exhibits small viscosity values. The shear thickening behavior is noted in a variety of polymer solutions, such as aqueous solutions of high-molecular-weight poly(ethylene oxide) (PEO),[2] and particulate systems, such as fumed silica suspensions in polyethylene glycol[3,4] and polymethylmethacrylate particles in glycerin–water mixtures.[5] In such systems, the shear-thickening behavior is attributed to the shear-induced aggregation of chains, due to their hydrophobicity (such as the aggregation of PEO chains in aqueous environments[2,6] or aqueous rod-like micellar solutions[7]), or due to the dominance of hydrodynamic forces over interparticle repulsive forces leading to the formation of particle aggregates in the case of suspensions;[8–10] the structure formed is referred to as a shear-induced structure (SIS).[6] Under equilibrium conditions, no attractive forces are acting on the particles, meaning that the suspension is comprised of primary particles (i.e., no aggregates). STFs have attracted considerable attention over the past few decades due to their emerging importance in dampers,[11,12] body armor,[4,9,13] medical equipment to prevent injuries,[8] as shields against high-velocity micrometeoroid/orbital debris impacts on spacecraft operating in the near-Earth space environment,[14] self-consolidating concrete,[15] and enhanced oil recovery.[16] However, the proper tailor-design of STFs to address these specific commercial applications necessitates the availability of a constitutive equation that accurately predicts their rheological behavior.

From a theoretical standpoint, several phenomenological models that provide a particular shear-rate dependency of the shear viscosity have been proposed that are fully parameterized using available experimental data (e.g., Refs. 17 and 18). However, these models usually provide expressions for the shear viscosity alone and ignore normal stresses. One of the first models to account for the effect of shear-thickening on both the shear stress and the normal stress differences is the Bautista–Manero–Puig (BMP) model[19] that coupled the Oldroyd-B model with the kinetic (fluidity) equation proposed by Fredrickson.[20] The BMP model was later extended,[21,22] via the use of extended irreversible thermodynamics (EIT),[23] to accommodate both the shear-thickening and shear-thinning behaviors. However, in these generalized BMP models, kinetic parameters rely empirically on the second invariants of the deformation rate and shear stress tensors. More recently, Tamano *et al.*[24] coupled the Giesekus and FENE-P

Published under an exclusive license by AIP Publishing

models with Fredrickson's kinetic equation; the use of the anisotropic Giesekus parameter in the former allowed for the prediction of a non-vanishing second normal stress coefficient. Both normal stress coefficients have been predicted to shear thicken followed by a shear thinning behavior. Possibly, the first thermodynamically admissible model for STFs is the one proposed by Edwards and co-workers[25,26] who employed the two-coupled Maxwell modes (TCMM) model[27] derived using the generalized bracket formalism[28] of non-equilibrium thermodynamics (NET).[28–31] In this model, two conformation tensors were considered: one characterizing the conformation of dissolved polymer chains and one that is associated with the SIS formed under shear and correlates with their size. The coupling between these two conformation tensors is controlled by an interaction parameter, and both tensors are considered to deform linearly (as Hookean dumbbells).[27] This model has been shown to compare favorably against available viscosity and dichroism data.

In this work, we will employ NET to develop a simple mathematical model addressing the rheological behavior of STFs, primarily shear-thickening polymer solutions (STPSs); in particular, we aim to show that the models using the fluidity methodology (such as the ones proposed in Refs. 19, 21, 22, and 24) are not thermodynamically admissible unless certain corrections are added to them. To accomplish this, we will develop the model using the Generalized bracket formalism[28] of NET,[28–31] by means of which several microstructured systems have been addressed, such as polymer melts and solutions,[28–30,32,33] polymer nanocomposites,[34,35] micellar systems,[36,37] blood,[38–40] drilling fluids,[41] and thixotropic fluids.[42] Thus, we guarantee that the model derived will be consistent with the law of thermodynamics as extended for beyond equilibrium systems. Also, we guarantee that the coupling between the various variables is accomplished self-consistently. The customarily employed methodology to derive constitutive models is to add terms to state variables' evolution equations, such as the conformation tensor and the scalar structural variable that we are to introduce in Sec. II, and the stress tensor without necessarily considering whether these additions should be done in a self-consistent way. In other words, a term added to the stress tensor should dictate the term to be added in, say, the scalar structural variable evolution equation, and not to be independent of it. In complete disaccord to this usual practice, in our approach, this is done automatically via the use of a non-equilibrium thermodynamics formalism.

The paper is structured as follows: in Sec. II, the new model is introduced, whereas Sec. III presents the model predictions along with a comparison with available rheological data. The paper concludes with Sec. IV where we elaborate on the significance of our work and future plans are highlighted and discussed.

II. METHODOLOGY

A. The vector of state variables

Throughout this work, we consider an isothermal and incompressible flow, meaning that both the mass density of polymer segments, ρ, and the entropy density (or temperature) are excluded from the vector of state variables. To describe the rheology and microstructure of the polymer segments, we follow previous works[39,40,43] and use a contravariant second-rank conformation tensor density defined as $\mathbf{C} = \rho\mathbf{c}$ to characterize the deformation of polymer segments, modeled as elastic dumbbells. Here, $\mathbf{c} = \int \mathbf{R}\mathbf{R}\psi(\mathbf{R}, t)d^3\mathbf{R}$ is the second moment of the distribution function $\psi(\mathbf{R}, t)$ for the end-to-end connector vector $\mathbf{R}$.[28–30,32,33] To account for the shear-thickening behavior, we need to employ one additional scalar structural variable, λ, to properly characterize the SIS formed when these segments aggregate at sufficiently high shear rates. At equilibrium, no SIS is noted, that is, only free polymer segments in polymer solutions or particles in suspensions exist, meaning that $\lambda = 0$, whereas as the shear rate increases the scalar structural variable should increase, as the SIS is gradually formed, reaching eventually to a constant value, λ_∞. Thus, λ accounts for the number of segments that are attached to the SIS relative to the number of all segments. To mention just one example, as the shear rate is increased, randomly oriented short rod-like micelles merge to form longer rod-like micelles.[7] Since, in this case, the merging leads to an increase in the length of the rod-like micelles, which can be monitored as a function of the shear rate, the rescaling of the length could be an indirect way of obtaining λ experimentally. On the other hand, it can very easily and directly be accessed via the use of non-equilibrium molecular dynamics simulations, either coarse-grained, such as the work of Castillo–Tejas and Manero,[44] or using a combined approach based on coarse-grained simulations followed be reverse-mapped all-atom molecular dynamics simulations.[45] Finally, we consider the momentum density $\mathbf{M}$ as the hydrodynamic variable, so that overall the vector $\mathbf{x}$ of state variables is expressed as $\mathbf{x} = \{\mathbf{M}, \mathbf{c}, \lambda\}$. Note that as the mass density of polymer segments is constant, due to incompressibility, we may employ the conformation tensor $\mathbf{c}$ directly.

B. The resulting evolution equations

The complete derivation is presented as supplementary material. The final evolution equations for each structural variable are as follows:

$$\dot{\tilde{\mathbf{c}}}_{[1]} = -\frac{1}{\tau_R(\lambda)}\left[\alpha h^2(\mathrm{tr}\tilde{\mathbf{c}})\tilde{\mathbf{c}}\cdot\tilde{\mathbf{c}} + h(\mathrm{tr}\tilde{\mathbf{c}})(1-2a)\tilde{\mathbf{c}} - (1-a)\mathbf{I}\right], \quad (1a)$$

$$\frac{D\lambda}{Dt} = \frac{\partial\lambda}{\partial t} + \mathbf{u}\cdot\nabla\lambda = \frac{1}{\tau_\lambda}\ln(1-\lambda) + (\lambda_\infty - \lambda)(\nabla\mathbf{u})^T : \tilde{\mathbf{c}}, \quad (1b)$$

where $\nabla\mathbf{u}$ is the velocity gradient tensor ($\mathbf{X}^T$ is the transpose of $\mathbf{X}$), $\dot{\gamma} \equiv \nabla\mathbf{u} + (\nabla\mathbf{u})^T$ is the rate-of-strain tensor, and $\mathbf{I}$ is the unit tensor. The left-hand side (LHS) of Eq. (1a) is the upper-convected time derivative, defined in supplementary material, Eq. (SM.6c), whereas the right-hand side (RHS) is the relaxation term aiming to relieve stress and thus bring the conformation tensor back to its equilibrium value, once the applied flow is ceased. The LHS of Eq. (1b) defines the material time derivative, whereas the first term in the RHS is the relaxation term of λ that accounts for the breakup of the SIS, and the second term accounts for the increase of the scalar structural variable with the imposed flow as a result of the buildup of the SIS. We should here stress that the precise form of the second term in the evolution equation of λ has been chosen by selecting the tensor $\mathbf{g}$, first appearing in the Poisson bracket given in supplementary material, Eq. (SM.4b), to closely match the corresponding term in the fluidity evolution equation, see Eq. (4). By making this selection, the precise form of the corresponding term in the stress tensor expression, last term in supplementary material, Eq. (SM.7), involving the $\mathbf{g}$ tensor is automatically specified [note that its form cannot be chosen arbitrary but should obey the constraints imposed by supplementary material, Eq. (SM.4c), so that the Poisson bracket satisfies the Jacobi identity; a check whether the Poisson bracket fulfills the Jacobi identity can also

Published under an exclusive license by AIP Publishing

be done using a computer-assisted method[46]]. As such, this additional term in the stress tensor expression, the second term in the square brackets in Eq. (2) below, is obtained in a self-consistent manner, without ambiguities, in complete disaccord to the usual practice, wherein the terms added in the various equations (evolution equations and the stress tensor equation) are introduced independently. Also, $h(\mathrm{tr}\tilde{\mathbf{c}}) = (b-3)/(b-\mathrm{tr}\tilde{\mathbf{c}})$ is the spring force law for finite-extensible dumbbells with b the extensibility parameter (the dimensionless maximum length of the chain) defined as $b = 3L^2/\langle R^2\rangle_{eq}$, with L denoting the maximum length of the chain and $\langle R^2\rangle_{eq}$ the mean square chain end-to-end distance at equilibrium. For given polymer chemistry, the extensibility parameter should not be considered as an adjustable (free) parameter but rather as a known constant that can be calculated via $b = [3(0.82)^2/C_\infty](M/M_0)$ where C_∞ is the polymer characteristic ratio, M the molecular weight, and M_0 the average molar mass per backbone bond, which is equal to half the monomer molecular weight. When the polymer is entangled, the entanglement molecular weight, M_e, should be used instead of the molecular weight.[47,48] Also, α is the second-order (Giesekus) anisotropic parameter[28,32,33,49,50] that determines the degree of anisotropy of the frictional properties as first proposed by Giesekus;[50] the consideration of a non-vanishing anisotropic parameter permits, as is to be illustrated below, the prediction of a non-vanishing second normal stress coefficient. Furthermore, $\tilde{\mathbf{c}} = (3/\langle R^2\rangle_{eq})\mathbf{c}$ is the dimensionless conformation tensor, λ_∞ is the maximum value of the scalar structural variable, and $\tau_R(\lambda) = \tau_{R,eq}/(1-\lambda)$ and τ_λ are the polymer chain deformation relaxation time and the breakup relaxation time, respectively. The former controls the deformation of the polymer segments, whereas the latter controls the breakup of the SIS as the shear rate decreases. In the following, we consider $\tau_\lambda = \varepsilon\tau_{R,eq}$, where the parameter ε quantifies the relative importance between the breakup and the flow-induced buildup of the SIS. When $\varepsilon \to 0$, the time needed for the breakup is much smaller than the one needed for the buildup of the SIS leading to a vanishing scalar structural variable, $\lambda \to 0$, and shear-thickening will not occur. On the other hand, when $\varepsilon \gg 1$, the time needed for the breakup is much larger than the one needed for the buildup of the SIS, meaning that the SIS will occur instantaneously, that is, $\lambda \to 1$. Thus, the appearance or not of a shear-thickening behavior is controlled by the parameter ε. Finally, the stress tensor is given as

$$\boldsymbol{\sigma} = \eta_s\dot{\boldsymbol{\gamma}} + \boldsymbol{\sigma}^p = \eta_s\dot{\boldsymbol{\gamma}} + G\left\{\left[h(\mathrm{tr}\tilde{\mathbf{c}}) - \frac{1}{2}(\lambda_\infty-\lambda)\ln(1-\lambda)\right]\tilde{\mathbf{c}} - \mathbf{I}\right\}. \quad (2)$$

Here, $\boldsymbol{\sigma}^p$ is the polymer stress tensor, η_s is the viscosity of the solvent, and $G = nk_BT$ is a (constant) elastic modulus, where n is the number density of polymer chains, k_B is Boltzmann's constant, and T is the absolute temperature. Note that the proof of the thermodynamic admissibility of the proposed constitutive model is presented in the supplementary material.

In total, we need to specify five parameters:

(1) The extensibility parameter, b (the dimensionless maximum length of the chain); for given polymer chemistry, the extensibility parameter should not be considered as an adjustable (free) parameter but rather as a known constant. For example, in the case of polystyrene (PS) $b = M/(248\ \mathrm{g/mol})$ where M is the polymer molecular weight.[47]
(2) The second-order (Giesekus) anisotropic parameter, α, that allows for the prediction of a non-vanishing second normal stress coefficient; as such, as usually these are not available experimentally we could set $\alpha = 0$, as we will do in Sec. III B.
(3) The parameter ε that quantifies the relative importance between the breakup and the flow-induced buildup of the SIS; equivalently, we could have used as a parameter the breakup relaxation time, $\tau_\lambda = \varepsilon\tau_{R,eq}$, of the SIS. This parameter could be assessed experimentally by first applying a shear rate sufficient for the formation of the SIS, such as the merging of short rod-like micelles into longer ones,[7] and then monitor the time-dependent relaxation of λ toward its equilibrium value once flow has ceased. The corresponding characteristic time obtained from this relaxation curve could be identified with τ_λ.
(4) The maximum value of the structural variable, λ_∞, which for simplicity could be considered to be equal to unity.
(5) The elastic modulus, $G = nk_BT$, which is proportional to the polymer concentration

Furthermore, the following parameters that are needed can be obtained directly from the rheological measurements:

(1) The polymer concentration, C_s, which is available from the sample that has been rheologically measured.
(2) The viscosity of the solvent, η_s, can be obtained directly from the sample used in the rheological experiments.
(3) The polymer viscosity at equilibrium, $\eta_{p,eq}$, can also be obtained directly from the sample used to perform the rheological experiments, via $\eta_{p,eq} = \eta_0 - \eta_s$, where η_0 is the zero-rate shear viscosity.
(4) The polymer chain equilibrium relaxation time, $\tau_{R,eq}$, can be obtained from the equation $\tau_{R,eq} = \eta_{p,eq}/G$. Note that via the use of atomistic simulations, $\tau_{R,eq}$ can be easily obtained through the orientational autocorrelation function of the end-to-end vector of the polymer chain, see, for example, Ref. 51.

C. Comparison with other models using the fluidity notion

It is important to elaborate as to how the new constitutive model for STPSs, as derived here in the context of the generalized bracket formalism of NET, compares with previously proposed models using the fluidity methodology.[19,21,22,24] To do this, we first write down the evolution equation of the polymer stress tensor by using Eq. (2) in Eq. (1a):

$$\begin{aligned}&\tau_R\dot{\boldsymbol{\sigma}}^p_{[1]} + \left[h(\mathrm{tr}\tilde{\mathbf{c}}) + f(\lambda)\right]\left(\boldsymbol{\sigma}^p + \frac{\alpha}{G}\boldsymbol{\sigma}^p\cdot\boldsymbol{\sigma}^p\right)\\ &\quad + \tau_R(\boldsymbol{\sigma}^p + G\mathbf{I})\frac{D\ln\left[h(\mathrm{tr}\tilde{\mathbf{c}}) + f(\lambda)\right]}{Dt}\\ &\quad + Gf(\lambda)\left[h(\mathrm{tr}\tilde{\mathbf{c}}) + f(\lambda)\right]\tilde{\mathbf{c}} - \alpha f(\lambda)\\ &\quad \times\left[Gf(\lambda)\tilde{\mathbf{c}}\cdot\tilde{\mathbf{c}} - \tilde{\mathbf{c}}\cdot\boldsymbol{\sigma}^p - \boldsymbol{\sigma}^p\cdot\tilde{\mathbf{c}}\right] = \tau_R G\dot{\boldsymbol{\gamma}}, \end{aligned} \quad (3)$$

where we have considered $f(\lambda) = -\frac{1}{2}(\lambda_\infty-\lambda)\ln(1-\lambda)$, and, following Refs. 19, 21, 22, and 24, the product $\eta_p = G\tau_R$ as a polymer viscosity and $\eta_{p,eq} = G\tau_{R,eq}$ its equilibrium value. Note that the evolution equation is not independent of the conformation tensor. According to the fluidity methodology,[19,21,22,24] the relaxation time is given as

Published under an exclusive license by AIP Publishing

$\tau_R = (G\varphi)^{-1}$ where φ is the fluidity (equal to the inverse polymer viscosity). The equilibrium relaxation time is thus given as $\tau_{R,eq} = (G\varphi_0)^{-1}$ where φ_0 is the zero-rate fluidity. Thus, given these two expressions for τ_R, the following relation between the scalar structural variable employed in our model and the fluidity can be obtained: $\varphi^* = \varphi/\varphi_0 = 1 - \lambda$. As such, the evolution equation for λ, Eq. (1b), can be written as an evolution equation for the fluidity:

$$\frac{D\varphi}{Dt} = -\frac{\varphi_0}{\tau_\lambda}\ln(\varphi/\varphi_0) + \frac{(\varphi_\infty - \varphi)}{G\left[h(\mathrm{tr}\tilde{\mathbf{c}}) + f(\lambda)\right]}(\nabla\mathbf{u})^T : \tilde{\mathbf{c}}, \tag{4a}$$

where $\varphi_\infty = \varphi_0(1 - \lambda_\infty)$ is the minimum value of the fluidity. By linearizing, we finally get

$$\frac{D\varphi}{Dt} = \frac{\varphi_0 - \varphi}{\tau_\lambda} + \frac{(\varphi_\infty - \varphi)}{G\left[h(\mathrm{tr}\tilde{\mathbf{c}}) + f(\lambda)\right]}(\nabla\mathbf{u})^T : \tilde{\mathbf{c}}. \tag{4b}$$

This is the same expression as the one customarily employed by researchers invoking the fluidity methodology. Note, however, that the appearance of the term $h(\mathrm{tr}\tilde{\mathbf{c}}) + f(\lambda)$ in the denominator of the second term is not found in their expression. Finally, we may also rewrite Eq. (3) as

$$\begin{aligned}&\frac{\tau_{R,eq}}{\varphi^*}\overset{p}{\underset{[1]}{\dot{\boldsymbol{\sigma}}}} + \left[h(\mathrm{tr}\tilde{\mathbf{c}}) + f(\lambda)\right]\left(\boldsymbol{\sigma}^p + \frac{\alpha}{G}\boldsymbol{\sigma}^p\cdot\boldsymbol{\sigma}^p\right)\\ &\quad + \frac{\tau_{R,eq}}{\varphi^*}(\boldsymbol{\sigma}^p + G\mathbf{I})\frac{D\ln\left[h(\mathrm{tr}\tilde{\mathbf{c}}) + f(\lambda)\right]}{Dt}\\ &\quad + Gf(\lambda)\left[h(\mathrm{tr}\tilde{\mathbf{c}}) + f(\lambda)\right]\tilde{\mathbf{c}} - \alpha f(\lambda)\\ &\quad \times\left[Gf(\lambda)\tilde{\mathbf{c}}\cdot\tilde{\mathbf{c}} - \tilde{\mathbf{c}}\cdot\boldsymbol{\sigma}^p - \boldsymbol{\sigma}^p\cdot\tilde{\mathbf{c}}\right] = \frac{\eta_{p,eq}}{\varphi^*}\dot{\boldsymbol{\gamma}}.\end{aligned} \tag{5}$$

Except for the extra terms related to the function $f(\lambda)$ that arise as a result of the self-consistency of our methodology relative to the fluidity methodology, Eq. (5) is identical to the one obtained using the fluidity methodology. In particular, when $\alpha = 0$ and $h = 1$ (Hookean dumbbells), we obtain the BMP model; when $\alpha = 0$, we obtain the f-FENE model;[24] and when $h = 1$, we obtain the f-Giesekus model.[24] As such, our approach provides the proper evolution equation when both anisotropic and finite extensibility effects are concurrently considered. Altogether, our present NET approach explicitly and unequivocally states that the BMP model,[19] as well as its generalizations,[21,22,24] is not thermodynamically admissible unless additional terms, concerning the function $f(\lambda)$ in Eqs. (4) and (5), are introduced.

We should here clarify that Manero *et al.*[21] also claim their model to be thermodynamically admissible via the use of EIT. In our present work, we have employed the Generalized bracket formalism of NET proposed by Beris and Edwards.[28] Alternatively, we could have also used the more general GENERIC formalism of Öttinger and Grmela.[29–31] The intrinsic difference between these two formalisms is the employment in the latter of two different generators, total energy, E, and total entropy, S, functionals, whereas only one, the Hamiltonian, is needed in the former; this fundamental difference does give more flexibility in the choice of the state variables.[29] Despite this, except for subtle issues in the case of systems described, for example, by the Boltzmann equation[52] (i.e., through the use of distribution functions as state variables) that favor GENERIC, the two formalisms are in complete agreement,[53] and may be used interchangeably. In these formalisms, the state variables comprise of the hydrodynamic ones, such as the momentum density, and of structural ones, such as the conformation tensor that relates to the microstructure of the system. On the other hand, in EIT the independent variables chosen are the fluxes, which are more macroscopic than the structural internal variables used by the two aforementioned formalisms.[54] Also, in EIT, like GENERIC and the Generalized bracket formalism, a non-equilibrium entropy expression is considered that depends on the independent variables, which comes directly from the requirement in EIT of a non-negative entropy production;[29] however, in EIT this is usually assumed to have a quadratic dependence on the independent variables. Jou and Casas-Vázquez[54] do mention that GENERIC and Generalized brackets provide, unlike EIT, a systematic methodology to derive non-equilibrium thermodynamic pressures. Overall, the Generalized bracket and GENERIC formalisms are not necessarily equivalent to EIT and are more appropriate to use beyond the second order of approximation in non-equilibrium perturbations.[54]

It should also be emphasized here that, as mentioned by Jou and Casas-Vázquez,[54] there is no counterpart of the Jacobi identity for the reversible dynamics in EIT, and the convected time derivatives are usually introduced rather than derived. Thus, in earlier works using EIT, the Jacobi identity is considered implicitly. On the other hand, when using the Generalized bracket or the GENERIC formalisms checking the Jacobi identity is a straightforward, albeit time-consuming, exercise. This difference is particularly important for our present work since the inconsistency between our derived model and the one of Manero *et al.*[21] lies exactly on the extra Poisson bracket considered, the second integral in supplementary material, Eq. (SM.4b), that includes the tensor $\mathbf{g}$ whose precise form is dictated through supplementary material, Eq. (SM.4c).

III. RESULTS

In this section, we consider homogeneous flows and present the predictions of the new model in the case of steady-state and startup simple shear, described by the kinematics $\mathbf{u} = (\dot{\gamma}y, 0, 0)$, and how they compare with available experimental data. The material functions to analyze are the shear viscosity $\eta = \sigma_{yx}/\dot{\gamma}$ and the two normal stress coefficients, $\Psi_1 = (\sigma_{xx} - \sigma_{yy})/\dot{\gamma}^2$ and $\Psi_2 = (\sigma_{yy} - \sigma_{zz})/\dot{\gamma}^2$. The results have been obtained by numerically solving the constitutive model, Eqs. (1a) and (1b), using MATLAB.

A. Material functions in simple shear flow

In Fig. 1, we depict the predictions of the structural variable λ as a function of the dimensionless shear rate, $\mathrm{Wi} = \tau_{R,eq}\dot{\gamma}$, for various values of the model parameters. We note that λ always approaches the value of λ_∞ at large shear rates irrespective of the values of the remaining model parameters. By increasing ε, we note that λ reaches the value of λ_∞ at smaller shear rates, whereas by increasing the anisotropic parameter it shifts to intermediate Wi, approximately between 0.2 and 10. The consideration of Hookean dumbbells, instead of FENE ones, is noted not to significantly affect λ.

Then, in Fig. 2 we depict the predictions of the steady-state dimensionless shear viscosity (without the solvent's contribution) as a function of the dimensionless shear rate for various values of the model parameters, while keeping $\alpha = 0$ [panel (a)] and $b = 100$ [panel (b)] fixed. In both panels, the black line depicts the model prediction when shear-thickening is not predicted, that is, when $\varepsilon \to 0$. In all cases, at small shear rates the shear viscosity reaches its low-rate value, $\eta_{p,eq} = G\tau_{R,eq}$. Concerning the predictions when $\alpha = 0$

Published under an exclusive license by AIP Publishing

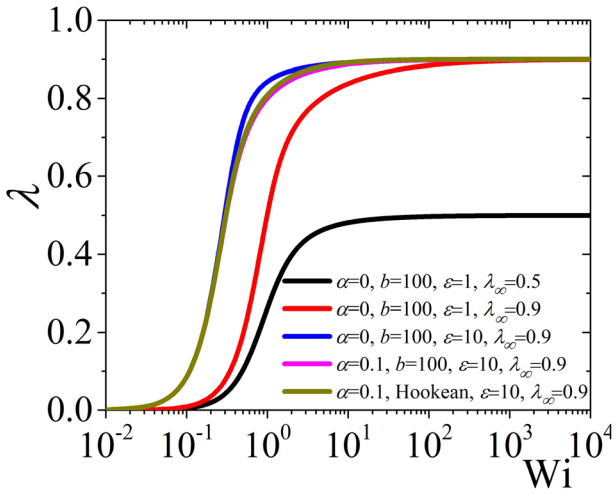

FIG. 1. Representative model predictions for the structural variable λ as a function of the dimensionless shear rate, Wi, for various values of the model parameters.

[panel (a)], we note that as ε is increased to unity the viscosity first shear thickens, reaching a maximum at Wi $\approx$ 2, and thereafter shear thins. Although the power-law behavior at large shear rates is the same as when $\varepsilon \to 0$, the curve is seen to shift upward slightly. By increasing the value of λ_∞, the shear-thickening behavior intensifies, whereas by increasing ε the shear-thickening behavior is presented at smaller shear rates and the position of the maximum shifts to about Wi $\approx$ 1 without affecting the prediction at large shear rates. When the force law is Hookean ($b \to \infty$) and $\alpha = 0$, the shear viscosity approaches a constant value at large shear rates, equal to $(1-\lambda_\infty)^{-1}$. Finally, when we increase the value of α, we note that the whole curve after about Wi $\approx$ 0.3 shifts downward [panel (b)]. Overall, the predictions concerning finite values of the finite extensibility parameter and $\alpha \neq 0$ are in line with available rheological measurements of STFs.[2,16,55]

In Fig. 3, we depict the predictions of the steady-state dimensionless first [panel (a)] and second [panel (b)] normal stress coefficient as a function of Wi for various values of the model parameters. In both panels, the black line depicts the model prediction when shear-thickening cannot be predicted, that is, when $\varepsilon \to 0$. We see that the behavior is similar to the one noted for the shear viscosity (Fig. 2). At small shear rates, they reach their low-rate values, that is, $\Psi_{1,0} = 2\tau_{R,eq}\eta_{p,eq}$ and $-\Psi_{2,0} = \alpha\tau_{R,eq}\eta_{p,eq}$. When considering a finite value of ε, both coefficients are noted to first shear thicken, reaching a maximum at about Wi $\approx$ 2, and then shear thin. For both normal stress coefficients, by increasing λ_∞ the shear thickening intensifies, whereas by increasing ε the position of the maximum shifts to Wi $\approx$ 1. When the value of α is increased, then Ψ_1 shifts downwards after about Wi $\approx$ 0.3, whereas the $-\Psi_2$ curve shift upwards. An interesting trend is that although the power-law behavior at large shear rates is the same as when $\varepsilon \to 0$, Ψ_1 is noted to shift upwards when λ_∞ increases and shifts downwards as α increases. On the contrary, the prediction of $-\Psi_2$ at large shear rates is the same irrespective of the model parameters. Finally, when the force law is Hookean ($b \to \infty$) and $\alpha = 0$, we then note that Ψ_1 approaches, following the behavior of the shear viscosity, at large shear rates a constant value, equal to $2(1-\lambda_\infty)^{-2}$.

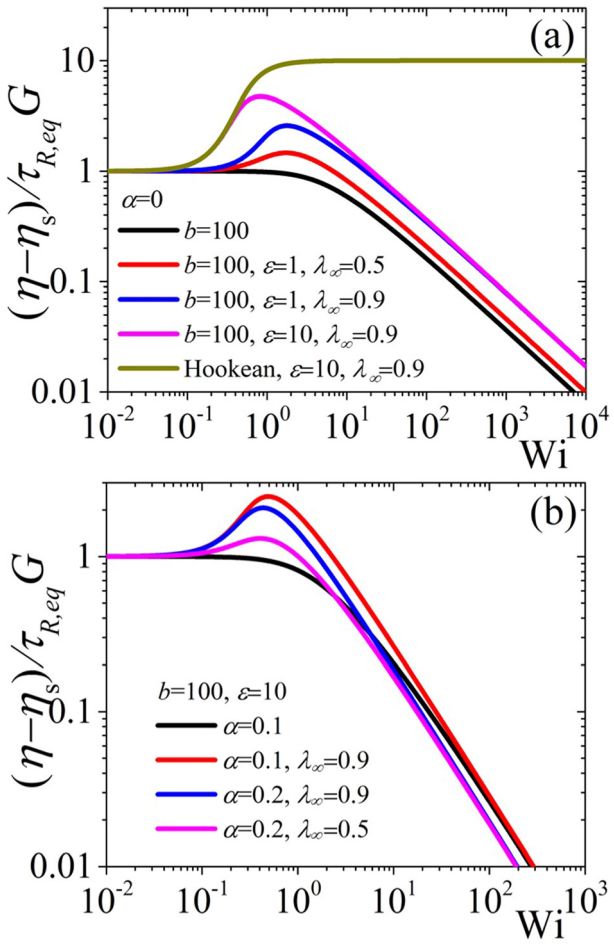

FIG. 2. Representative model predictions for the steady-state dimensionless shear viscosity, minus the solvent's contribution, as a function of the dimensionless shear rate, Wi, for various values of the model parameters. The following parameters are kept fixed: in (a) $\alpha = 0$ and (b) $b = 100$.

In Fig. 4, we present the model predictions for the growth of the shear viscosity, $\eta^+(t)$, and the two normal stress coefficients, $\Psi_1^+(t)$ and $\Psi_2^+(t)$, respectively, upon inception of shear flow at two different values of the dimensionless shear rate Wi (=1, and 10), along with the prediction of the linear viscoelastic (LVE) behavior (dotted orange line) given by Eq. (6):

$$\frac{\eta^+(t)-\eta_s}{\eta_{p,eq}} = 1-\exp\left(-\frac{t}{\tau_{R,eq}}\right),$$

$$\frac{\Psi_1^+(t)}{\tau_{R,eq}\eta_{p,eq}} = 2\left[1-\left(1+\frac{t}{\tau_{R,eq}}\right)\exp\left(-\frac{t}{\tau_{R,eq}}\right)\right],$$

$$\frac{-\Psi_2^+(t)}{\tau_{R,eq}\eta_{p,eq}} = \alpha\left\{1-\left(1+\frac{t}{\tau_{R,eq}}\right)\exp\left(-\frac{t}{\tau_{R,eq}}\right) + \exp\left(-\frac{t}{\tau_{R,eq}}\right)\left[1-\frac{t}{\tau_{R,eq}}-\exp\left(-\frac{t}{\tau_{R,eq}}\right)\right]\right\}. \quad (6)$$

Published under an exclusive license by AIP Publishing

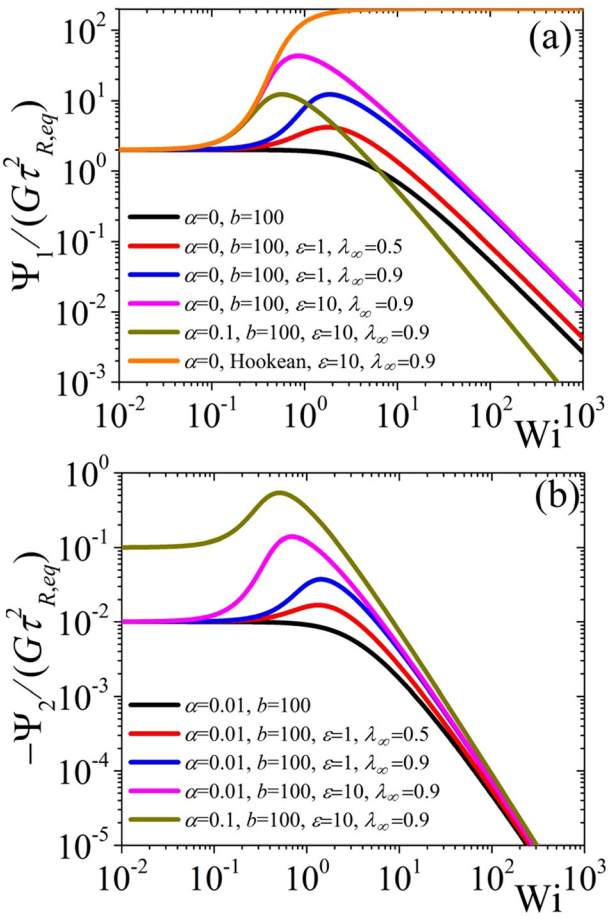

FIG. 3. Same as Fig. 2 but for the steady-state dimensionless (a) first normal stress coefficient, and (b) second normal stress coefficient.

We note that irrespective of the shear rate and the values of the parameters considered, at sufficiently short times, all viscometric curves follow the LVE prediction, which is the expected theoretical prediction. At small shear rates (Wi = 1), we note that all three material functions are seen to approach their steady-state values monotonically when $\varepsilon = 0$.[32,33] On the other hand, when $\varepsilon > 0$, an overshoot is noted, which intensifies as ε increases. Also, all viscometric curves are noted to reach to steady-state values that are larger than those when $\varepsilon = 0$, which is the expected outcome of the shear-thickening behaviour occurring at these shear rate, cf. Figs. 2 and 3. As the shear rate increases (Wi = 10), the non-shear-thickening fluids are noted to go through an overshoot before they reach to their steady-state values.[32,33] The shear-thickening fluids are noted to exhibit a more intense overshoot, but their shear viscosity and first normal stress coefficient also go through an undershoot right after the overshoot. Both $\eta^+(t)$ and $\Psi_1^+(t)$ are noted to go over (instead of below) the LVE predictions. Finally, the behavior of the transient second normal stress coefficient is noted to be more complicated as it does not seem to follow the LVE envelope at small-to-intermediate times.

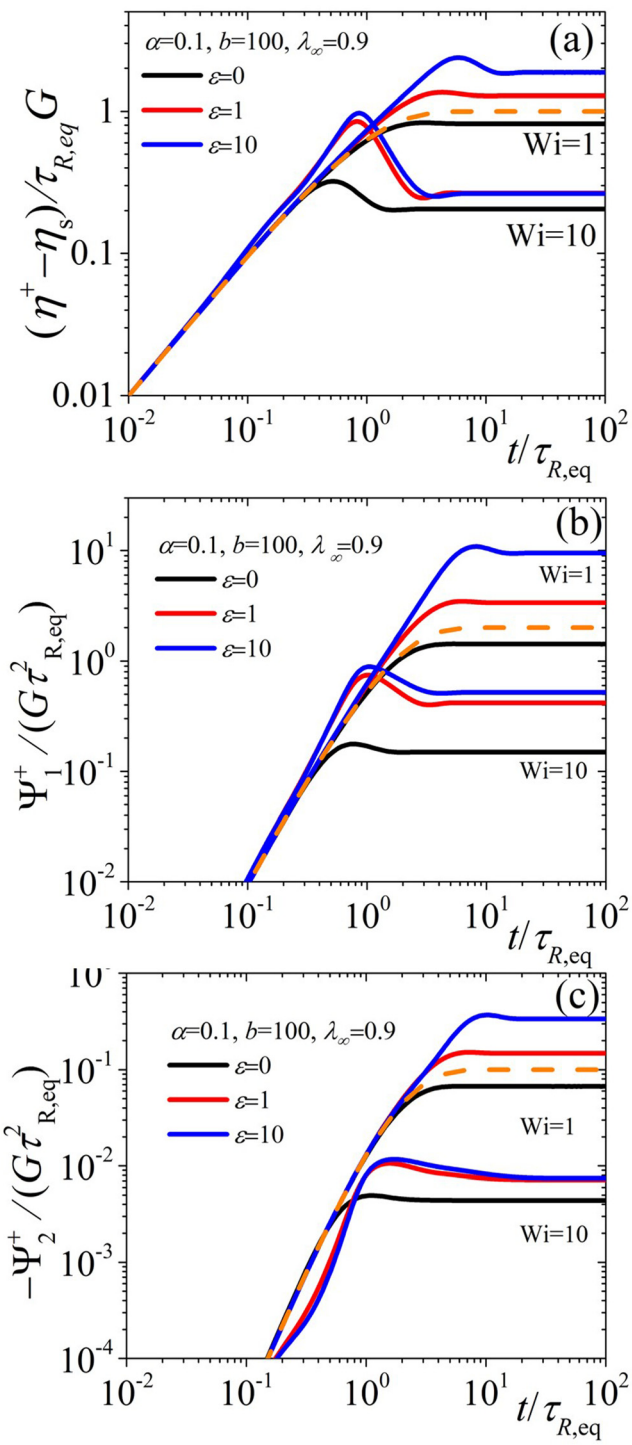

FIG. 4. Growth of the transient dimensionless (a) shear viscosity, and the (b) first and (c) second normal stress coefficients upon inception of shear flow at different dimensionless shear rates (Wi = 1 for the uppermost curves, and Wi = 10 for the lower ones) for several values of ε when keeping $\alpha = 0.1, b = 100, \lambda_\infty = 0.9$ constant. The LVE envelope is depicted as a dashed orange line.

Published under an exclusive license by AIP Publishing

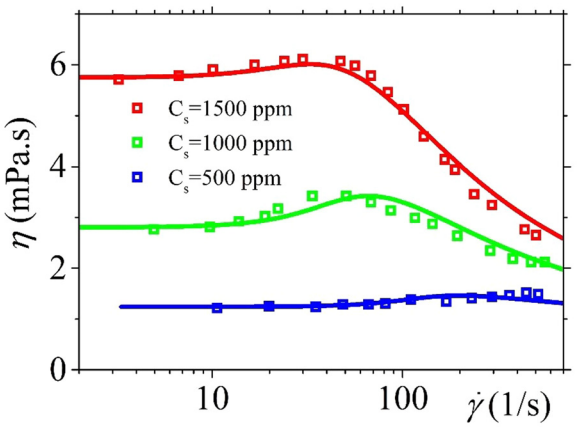

FIG. 5. Comparison of the model predictions for the shear viscosity with the experimental rheological data of three ODMAO solutions.[55]

B. Comparison with experimental data

Next, we validate the capacity of the derived model to compare with available experimental measurements. Figure 5 presents a comparison between model predictions and experimental data[55] on the shear viscosity of a dilute aqueous (thus $\eta_s = 1$ mPa s) nonionic surfactant, mainly consisted of oleyl-dimethylamine oxide [ODMAO, $C_{18}H_{37}N(CH_3)_2O$], solutions for different ODMAO concentrations $C_s = 500, 1000$, and 1500 ppm at $T = 20\,^{\circ}$C. Since no data for $-\Psi_2$ are available, we consider $\alpha = 0$, and for simplicity, we consider $\lambda_\infty = 1$. As no information pertinent to the calculation of the extensibility parameter of ODMAO can be found, we will consider it here as an adjustable parameter; given the small size of ODMAO chains, we consider $b = 5$. The elastic modulus is given via $G = G_0 C_s$ with $G_0 = 0.12$ mPa. The value of the polymer viscosity at equilibrium, $\eta_{p,eq}$, is obtained directly from the zero-rate shear viscosity via $\eta_{p,eq} = \eta_0 - \eta_s$, whereas $\tau_{R,eq}$ is obtained via $\tau_{R,eq} = \eta_{p,eq}/G$. The only remaining parameter to specify is ε. The selected values of $\eta_{p,eq}$, G, $\tau_{R,eq}$, and ε for each ODMAO solution are depicted in Table I. The comparison, presented in Fig. 5, shows that the model is capable of reproducing the rheological data quite well.

IV. CONCLUSIONS

During the past few decades, there has been a widespread interest in understanding the rheological behavior of shear-thickening fluids that stems from their increasing applicability in numerous commercial applications, from body armor to injury-preventing medical equipment. Given the tremendous span of their commercial applications, it is necessary to tailor-design each STF to properly address all engineering issues related to each application. Thus, it is essential to have a rheological model that adequately addresses their distinct rheological footprint.

TABLE I. Values of the parameter selected to fit the experimental data depicted in Fig. 5.

C_s (ppm)	$\eta_{p,eq}$ (mPa s)	G (mPa)	$\tau_{R,eq}$ (s)	ε
500	0.24	60	4.00×10^{-3}	5
1000	1.80	120	1.50×10^{-2}	1.5
1500	4.75	180	2.64×10^{-3}	0.5

We have herein introduced such a constitutive model for shear-thickening polymer solutions that is derived via the use of non-equilibrium thermodynamics, allowing therefore for the proper coupling between the two structural variables, the conformation tensor and the scalar structural variable λ, with each other and with the flow field and consistency with the thermodynamic laws. To the best of the author's knowledge, the present model is the first to include two structural variables (one tensorial and one scalar) and is developed using NET, employing the more general generalized bracket[28] formalism, except for the use of EIT by Manero *et al.*[21] and Landázuri *et al.*[22] However, we show that our NET approach explicitly and unequivocally states that the BMP model[19] and its generalizations[21,22,24] are *not* thermodynamically admissible unless specific amendments to their functional form are undertaken. As such, the model proposed in this work, Eqs. (4a) and (5), should be employed in the future.

We have showcased that the model can predict the shear viscosity of dilute nonionic surfactant (ODMAO) solutions.[55] Furthermore, we have shown that, in addition to the shear viscosity, the first and second normal stress coefficients also shear thicken, in line with previous works.[24] However, we have been unable to judge whether this behavior is a physical one since no such rheological data are available.

We do admit that the current version of our model bears certain limitations. At first, various rheological measurements show that some STFs first shear-thin before shear-thicken.[3,4,56] The present version of the model is unable of reproducing this behavior. This may be amended by considering coupling terms between the structural variables, which we have currently omitted for mere simplicity. Second, currently the model only accommodates the aggregation of polymer segments. To accommodate for the existence of particles in suspensions, we need to add to the vector of state variables the orientation tensor, following our previous work on suspension rheology.[34,35] In the context of rod-like particles, the scalar structural variable could be considered to be the scaled length of the rods that increases under flow, as done by Dutta and Graham.[57] We plan to undertake this generalization in a future publication.

SUPPLEMENTARY MATERIAL

See the supplementary material for the complete model derivation using non-equilibrium thermodynamics and a proof of its thermodynamic admissibility.

ACKNOWLEDGMENTS

The author thanks Mr. Emmanuel N. Skountzos for suggesting the modeling of shear-thickening fluids.

DATA AVAILABILITY

The data that support the findings of this study are available from the author upon reasonable request.

REFERENCES

[1]R. B. Bird, R. C. Armstrong, and O. Hassager, *Dynamics of Polymeric Liquids*, Fluid Mechanics Vol. 1 (Wiley-Interscience, 1977).

Published under an exclusive license by AIP Publishing

[2]D. Rivero, L. M. Gouveia, A. J. Müller, and A. E. Sáez, "Shear-thickening behavior of high molecular weight poly(ethylene oxide) solutions," Rheol. Acta **51**, 13 (2012).
[3]Q. M. Wu, J. M. Ruan, B. Y. Huang, Z. C. Zhou, and J. P. Zou, "Rheological behavior of fumed silica suspension in polyethylene glycol," J. Cent. South Univ. Technol. **13**, 1 (2006).
[4]M. Hasanzadeh, V. Mottaghitalab, H. Babaei, and M. Rezaei, "The influence of carbon nanotubes on quasi-static puncture resistance and yarn pull-out behavior of shear-thickening fluids (STFs) impregnated woven fabrics," Composites, Part A **88**, 263 (2016).
[5]W. Jiang, Y. Sun, Y. Xu, C. Peng, X. Gong, and Z. Zhang, "Shear-thickening behavior of polymethylmethacrylate particles suspensions in glycerine-water mixtures," Rheol. Acta **49**, 1157 (2010).
[6]C. H. Liu and D. J. Pine, "Shear-induced gelation and fracture in micellar solutions," Phys. Rev. Lett. **77**, 2121 (1996).
[7]M. Takeda, T. Kusano, T. Matsunaga, H. Endo, M. Shibayama, and T. Shikata, "Rheo-SANS studies on shear-thickening/thinning in aqueous rodlike micellar solutions," Langmuir **27**, 1731 (2011).
[8]J. Ding, P. Tracey, W. Li, G. Peng, P. G. Whitten, and G. G. Wallace, "Review on shear thickening fluids and applications," Text. Light Ind. Sci. Technol. **2**, 161 (2013).
[9]S. Gürgen, M. C. Kuşhan, and W. Li, "Shear thickening fluids in protective applications: A review," Prog. Polym. Sci. **75**, 48 (2017).
[10]Y. F. Lee, Y. Luo, T. Bai, C. Velez, S. C. Brown, and N. J. Wagner, "Microstructure and rheology of shear-thickening colloidal suspensions with varying interparticle friction: Comparison of experiment with theory and simulation models," Phys. Fluids **33**, 033316 (2021).
[11]C. Fischer, A. Bennani, V. Michaud, E. Jacquelin, and J. A. E. Månson, "Structural damping of model sandwich structures using tailored shear thickening fluid compositions," Smart Mater. Struct. **19**, 035017 (2010).
[12]K. Lin, A. Zhou, H. Liu, Y. Liu, and C. Huang, "Shear thickening fluid damper and its application to vibration mitigation of stay cable," Structures **26**, 214 (2020).
[13]J. Qin, B. Guo, L. Zhang, T. Wang, G. Zhang, and X. Shi, "Soft armor materials constructed with Kevlar fabric and a novel shear thickening fluid," Composites, Part B **183**, 107686 (2020).
[14]J. Warren, M. Cole, S. Offenberger, K. R. Kota, T. E. Lacy, H. Toghiani, M. Burchell, S. Kundu, and C. U. Pittman, "Hypervelocity impacts on honeycomb core sandwich panels filled with shear thickening fluid," Int. J. Impact Eng. **150**, 103803 (2021).
[15]X. Wang, A. Lu, and K. Wang, "Effect of interparticle action on shear thickening behavior of cementitious composites: Modeling and experimental validation," J. Sustainable Cem. Mater. **9**, 78 (2020).
[16]F. Jiang and W. Pu, "Salt induced shear thickening behavior of a hydrophobic association polymer and its potential in enhanced oil recovery," J. Mater. Sci. **55**, 3130 (2020).
[17]T. Shende, V. J. Niasar, and M. Babaei, "An empirical equation for shear viscosity of shear thickening fluids," J. Mol. Liq. **325**, 115220 (2021).
[18]F. J. Galindo-Rosales, F. J. Rubio-Hernández, and A. Sevilla, "An apparent viscosity function for shear thickening fluids," J. Non-Newtonian Fluid Mech. **166**, 321 (2011).
[19]F. Bautista, J. M. De Santos, J. E. Puig, and O. Manero, "Understanding thixotropic and antithixotropic behavior of viscoelastic micellar solutions and liquid crystalline dispersions. I. The model," J. Non-Newtonian Fluid Mech. **80**, 93 (1999).
[20]A. G. Fredrickson, "A model for the thixotropy of suspensions," AIChE J. **16**, 436 (1970).
[21]O. Manero, J. H. Pérez-López, J. I. Escalante, J. E. Puig, and F. Bautista, "A thermodynamic approach to rheology of complex fluids: The generalized BMP model," J. Non-Newtonian Fluid Mech. **146**, 22 (2007).
[22]G. Landázuri, E. R. Macías, J. P. García-Sandoval, E. Hernández, O. Manero, J. E. Puig, and F. Bautista, "On the modelling of the shear thickening behavior in micellar solutions," Rheol. Acta **55**, 547 (2016).
[23]D. Jou, J. Casas-Vázquez, and M. Criado-Sancho, "Thermodynamics of fluids under flow," in *Thermodynamics of Fluids under Flow*, 2nd ed. (Springer, 2011).
[24]S. Tamano, S. Hamanaka, Y. Nakano, Y. Morinishi, and T. Yamada, "Rheological modeling of both shear-thickening and thinning behaviors through constitutive equations," J. Non-Newtonian Fluid Mech. **283**, 104339 (2020).
[25]B. Jiang, D. J. Keffer, B. J. Edwards, and J. N. Allred, "Modeling shear thickening in dilute polymer solutions: Temperature, concentration, and molecular weight dependencies," J. Appl. Polym. Sci. **90**, 2997 (2003).
[26]B. J. Edwards, D. J. Keffer, and C. W. Reneau, "An examination of the shear-thickening behavior of high molecular weight polymers dissolved in low-viscosity Newtonian solvents," J. Appl. Polym. Sci. **85**, 1714 (2002).
[27]B. J. Edwards, A. N. Beris, and V. G. Mavrantzas, "A Model with Two Coupled Maxwell Modes," J. Rheol. **40**, 917 (1996).
[28]A. N. Beris and B. J. Edwards, "Thermodynamics of flowing systems: With internal microstructure," in *Thermodynamics of Flowing Systems: With Internal Microstructure* (Oxford University Press, New York, 1994).
[29]H. C. Öttinger, "Beyond equilibrium thermodynamics," in *Beyond Equilibrium Thermodynamics* (John Wiley and Sons, 2005).
[30]H. C. Öttinger and M. Grmela, "Dynamics and thermodynamics of complex fluids. II. Illustrations of a general formalism," Phys. Rev. E **56**, 6633 (1997).
[31]M. Grmela and H. C. Öttinger, "Dynamics and thermodynamics of complex fluids. I. Development of a general formalism," Phys. Rev. E **56**, 6620 (1997).
[32]P. S. Stephanou, C. Baig, and V. G. Mavrantzas, "A generalized differential constitutive equation for polymer melts based on principles of nonequilibrium thermodynamics," J. Rheol. **53**, 309 (2009).
[33]P. S. Stephanou, I. C. Tsimouri, and V. G. Mavrantzas, "Simple, accurate and user-friendly differential constitutive model for the rheology of entangled polymer melts and solutions from nonequilibrium thermodynamics," Materials **13**, 2867 (2020).
[34]P. S. Stephanou, V. G. Mavrantzas, and G. C. Georgiou, "Continuum model for the phase behavior, microstructure, and rheology of unentangled polymer nanocomposite melts," Macromolecules **47**, 4493 (2014).
[35]P. S. Stephanou, "How the flow affects the phase behaviour and microstructure of polymer nanocomposites," J. Chem. Phys. **142**, 064901 (2015).
[36]N. Germann, L. P. Cook, and A. N. Beris, "Nonequilibrium thermodynamic modeling of the structure and rheology of concentrated wormlike micellar solutions," J. Non-Newtonian Fluid Mech. **196**, 51 (2013).
[37]P. S. Stephanou, I. C. Tsimouri, and V. G. Mavrantzas, "Two-species models for the rheology of associative polymer solutions: Derivation from nonequilibrium thermodynamics," J. Rheol. **64**, 1003 (2020).
[38]I. C. Tsimouri, P. S. Stephanou, and V. G. Mavrantzas, "A constitutive rheological model for agglomerating blood derived from nonequilibrium thermodynamics," Phys. Fluids **30**, 030710 (2018).
[39]P. S. Stephanou, "A constitutive hemorheological model addressing both the deformability and aggregation of red blood cells," Phys. Fluids **32**, 103103 (2020).
[40]P. S. Stephanou and I. C. Tsimouri, "A constitutive hemorheological model addressing the deformability of red blood cells in ringer solutions," Soft Matter **16**, 7585 (2020).
[41]P. S. Stephanou, "The rheology of drilling fluids from a non-equilibrium thermodynamics perspective," J. Pet. Sci. Eng. **165**, 1010 (2018).
[42]P. S. Stephanou and G. G. Georgiou, "A nonequilibrium thermodynamics perspective of thixotropy," J. Chem. Phys. **149**, 244902 (2018).
[43]P. S. Stephanou, "Erratum: 'A constitutive hemorheological model addressing both the deformability and aggregation of red blood cells' [Phys. Fluids **32**, 103103 (2020)]," Phys. Fluids **33**, 039901 (2021).
[44]J. Castillo-Tejas and O. Manero, "Molecular dynamics of shear banding flow in associative polymers solutions: Effect of sticker groups location," Rheol. Acta (2021).
[45]S. D. Peroukidis, D. G. Tsalikis, M. G. Noro, I. P. Stott, and V. G. Mavrantzas, "Quantitative prediction of the structure and viscosity of aqueous micellar solutions of ionic surfactants: A combined approach based on coarse-grained MARTINI simulations followed by reverse-mapped all-atom molecular dynamics simulations," J. Chem. Theory Comput. **16**, 3363 (2020).
[46]M. Kröger and M. Hütter, "Automated symbolic calculations in nonequilibrium thermodynamics," Comput. Phys. Commun. **181**, 2149–2157 (2010).
[47]P. S. Stephanou, I. C. Tsimouri, and V. G. Mavrantzas, "Flow-induced orientation and stretching of entangled polymers in the framework of nonequilibrium thermodynamics," Macromolecules **49**, 3161 (2016).

Published under an exclusive license by AIP Publishing

[48]R. G. Larson, "The structure and rheology of complex fluids," in *The Structure and Rheology of Complex Fluids* (Oxford University Press, New York, 1999).
[49]J. M. Kim, P. S. Stephanou, B. J. Edwards, and B. Khomami, "A mean-field anisotropic diffusion model for unentangled polymeric liquids and semi-dilute solutions: Model development and comparison with experimental and simulation data," J. Non-Newtonian Fluid Mech. **166**, 593 (2011).
[50]H. Giesekus, "A simple constitutive equation for polymer fluids based on the concept of deformation-dependent tensorial mobility," J. Non-Newtonian Fluid Mech. **11**, 69 (1982).
[51]D. G. Tsalikis, T. Koukoulas, V. G. Mavrantzas, R. Pasquino, D. Vlassopoulos, W. Pyckhout-Hintzen, A. Wischnewski, M. Monkenbusch, and D. Richter, "Microscopic structure, conformation, and dynamics of ring and linear poly(ethylene oxide) melts from detailed atomistic molecular dynamics simulations: Dependence on chain length and direct comparison with experimental data," Macromolecules **50**, 2565 (2017).
[52]B. J. Edwards, A. N. Beris, and H. C. Öttinger, "An analysis of single and double generator thermodynamic formalisms for complex fluids. II. The microscopic description," J. Non-Equilib. Thermodyn. **23**, 334 (1998), available at https://www.degruyter.com/document/doi/10.1515/jnet.1998.23.4.334/html.
[53]B. J. Edwards, "An analysis of single and double generator thermodynamic formalisms for the macroscopic description of complex fluids," J. Non-Equilib. Thermodyn. **23**, 301 (1998), available at https://www.degruyter.com/document/doi/10.1515/jnet.1998.23.4.301/html.
[54]D. Jou and J. Casas-Vázquez, "Extended irreversible thermodynamics and its relation with other continuum approaches," J. Non-Newtonian Fluid Mech. **96**, 77 (2001).
[55]S. Tamano, Y. Ohashi, and Y. Morinishi, "Dynamics of falling droplet and elongational properties of dilute nonionic surfactant solutions with drag-reducing ability," Phys. Fluids **29**, 053104 (2017).
[56]A. Bosco, V. Calado, and J. Maia, "Rheological parameters of shear-thickening fluids using an experimental design," Mater. Res. **22**, e20180631 (2019).
[57]S. Dutta and M. D. Graham, "Mechanistic constitutive model for wormlike micelle solutions with flow-induced structure formation," J. Non-Newtonian Fluid Mech. **251**, 97 (2018).

Published under an exclusive license by AIP Publishing